

# HELIOSPHERIC AND INTERSTELLAR PHENOMENA DEDUCED FROM PICKUP ION OBSERVATIONS

GEORGE GLOECKLER

*Department of Physics and IPST, University of Maryland, College Park, MD 20742, U.S.A. and  
Department of Atmospheric, Oceanic and Space Sciences, University of Michigan,  
Ann Arbor, MI 48109, U.S.A.*

JOHANNES GEISS

*International Space Science Institute, Hallerstrasse 6, 3012 Bern, Switzerland*

**Abstract.** Pickup ions, created by ionization of slow moving atoms and molecules well inside the heliosphere, provide us with a new tool to probe remote regions in and beyond the heliosphere and to study injection and acceleration processes in the solar wind. Comprehensive and continuous measurements of H, He, C, N, O, Ne and other pickup ions, especially with the Solar Wind Ion Composition Spectrometer (SWICS) on both *Ulysses* and ACE, have given us a wealth of data that have been used to infer chemical and physical properties of the local interstellar cloud. With SWICS on *Ulysses* we discovered a new population of pickup ions, produced from atomic and molecular sources deep inside the heliosphere. The velocity distributions and composition of these “inner source” pickup ions are distinctly different from those of interstellar pickup ions, showing effects of strong adiabatic cooling, and a composition resembling that of the solar wind. Strong cooling indicates that the source of these pickup ions lies close to the Sun. The similarity of composition of inner source heavy ions to that of the solar wind implies that the dominant production mechanism for these pickup ions involves the absorption and re-emission of solar wind from interplanetary dust grains. While interstellar pickup ions are the seed population of the main Anomalous Cosmic Rays (ACRs), inner source pickup ions may be an important source of the rarer ACRs such as C, Mg, Si, S, and Fe. We present new results and review previous work with an emphasis on characteristics of the local interstellar cloud and properties of the inner source.

## 1. Introduction

Pickup ions (PIs) are singly-charged particle populations in the heliosphere that originate from neutral material (atoms and molecules) inside the heliosphere. A dominant source of such neutral matter is the gas from the local interstellar cloud (LIC) that surrounds the solar system. It was believed in the early 1970s, based on our knowledge of the local interstellar medium and from all-sky UV maps, that neutral gas, consisting primarily of hydrogen and helium atoms, enters the heliosphere because of the relative motion ( $\sim 25 \text{ km s}^{-1}$ ) of the Sun with respect to the LIC, and penetrates within several AU from the Sun before much of it becomes ionized and is then swept out of the heliosphere (e.g., Axford, 1972, and references therein). The basic characteristics of interstellar pickup ions (IPIs) created



*Space Science Reviews* **97**: 169–181, 2001.

© 2001 Kluwer Academic Publishers. Printed in the Netherlands.

from these interstellar neutrals were predicted (Vasyliunas and Siscoe, 1976), and IPIs were proposed as the source of Anomalous Cosmic Rays (Fisk *et al.*, 1974). However, IPIs remained invisible until  $\text{He}^+$  was discovered at 1 AU with AMPTE (Möbius *et al.*, 1985), and  $\text{H}^+$  (Gloeckler *et al.*, 1993) and the heavy IPIs (Geiss *et al.*, 1994) beyond several AU with *Ulysses*. The unambiguous detection of PIs required a new generation of ion mass spectrometers such as the SWICS instrument on *Ulysses* (Gloeckler *et al.*, 1992) that could measure the mass per charge of ions and had low background.

While the discovery of IPIs had been anticipated, the discovery of another pickup ion population, the so called ‘inner source’ came as a complete surprise. The detection of singly ionized carbon at levels comparable to that of  $\text{O}^+$  (Geiss *et al.*, 1995) was contrary to expectations based on the hypothesis of interstellar gas as its source. Carbon is believed to be nearly completely ionized in the LIC and thus pickup  $\text{C}^+$  was predicted not to exist. A new source for  $\text{C}^+$ , proposed by Geiss *et al.* (1995), was neutral gas released from grains and dust from an extended region within a few AU from the Sun.

## 2. Pickup Ion Characteristics

Pickup ions are produced from slow moving (compared to the solar wind) neutrals by photo-ionization and charge exchange with the solar wind. They are singly charged, except for interstellar pickup He, approximately three percent of which is doubly ionized (Gloeckler *et al.*, 1997). Once ionized they are picked up by the solar wind’s convected magnetic field and are rapidly swept outward. In the pickup process slow moving, cold neutrals with typical energies of a few eV are accelerated to become fast moving hot pickup ions with an energy of several keV. This conversion of neutrals to PIs which is strongest close to the Sun, gradually removes these neutrals and plays an important role in determining their spatial distribution in the heliosphere. For interstellar atoms ionization reduces their density significantly at heliocentric distances less than several AU, except for He whose density remains fairly constant to about 0.5 AU before it begins to drop. Adiabatic cooling in the expanding solar wind affects PIs. Pickup ions lose energy as they move outward. Cooling is clearly observed in the velocity distributions of PIs, especially for inner source PIs produced predominantly close to the Sun. The maximum energy of newly created PIs is twice the ambient solar wind speed. However, in the turbulent solar wind IPIs are observed at higher speeds not only downstream of shocks but at other times as well (Gloeckler *et al.*, 2000a). This indicates that pickup ions (as well as other suprathermal ions) are readily accelerated in the turbulent solar wind.

Most of this was known long before IPIs were detected. The basic characteristics of IPIs were confirmed by observations of their velocity distributions such as those shown in Figure 1. The proton distribution (Figure 1a) is the most complicated of the two because it shows a mix of three  $\text{H}^+$  populations each of which

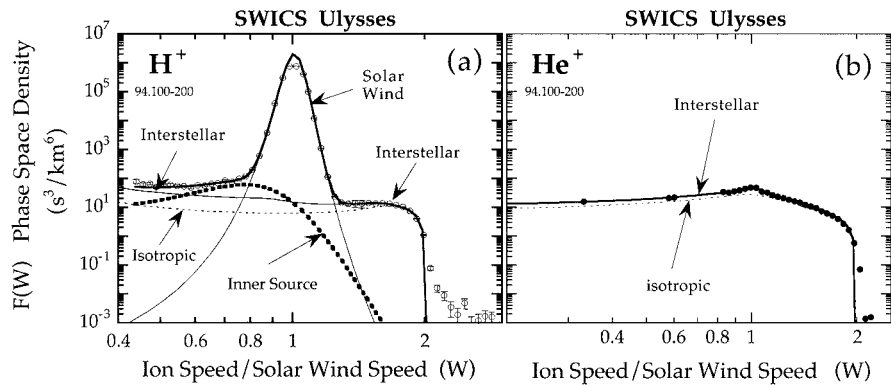


Figure 1. Velocity distribution function of  $H^+$  (a) and  $He^+$  (b) averaged over a 100-day period when *Ulysses* was at high latitude in the high speed stream. The phase space density was measured with the SWICS instrument as a function of  $W$  (ion speed/solar wind speed). The  $H^+$  spectrum contains several populations (solar wind, inner source and interstellar  $H^+$ ) as indicated in the figure.  $He^+$  is predominantly interstellar, with negligible contributions from the other two populations. The light dotted curves are model calculations of the phase space density assuming strong pitch angle scattering which produces isotropic velocity distributions in the reference frame of the solar wind. These curves are a poor fit to the data. Anisotropic distribution functions, which result from weak pitch angle scattering, provide a far better fit. Scattering mean free paths inferred from best fits to the observed spectra are 1 AU or more (Gloeckler *et al.*, 1995), much larger than was expected prior to these measurements.

dominates in a certain  $W$  (ion speed/solar wind speed) range: solar wind protons for  $W$  between  $\sim 0.8$  and  $\sim 1.3$ , inter-stellar  $H^+$  above  $W \approx 1.3$  and below  $\approx 0.6$ , and inner source  $H^+$  between  $\sim 0.6$  and  $\sim 0.8$ . The most prominent feature of the IPI spectra is the sharp drop-off in phase space density above the characteristic cutoff speed of  $W \approx 2$ , which was predicted and is clearly visible in both spectra. A sharp drop in density of IPIs at  $W \approx 2$  implies that a significant fraction of those IPIs is produced locally, at the location where the observations are made. Below the  $W \approx 2$  cutoff, the spectral shape of interstellar  $H^+$  is much flatter than that of  $He^+$ . This is due to the different ionization loss rates of atomic H and He which results in the respective different radial gradients of these two species. Because of adiabatic cooling the radial gradient of the parent atom is imprinted in the spectral shape of the PI. Thus, the spectral shape of IPIs can be used to infer the ionization loss rate of its parent atoms. From the distribution function of IPIs one can deduce not only the ionization rate but also the density of the parent atoms in the distant heliosphere (e.g., the termination shock).

The distribution functions of heavy PIs are shown in Figure 2. The spectrum at  $\sim 5$  AU of the rare  $Ne^+$  (right panel) demonstrates particularly well the contributions from both the inner ( $W < \sim 1.3$ ) and the interstellar ( $W > \sim 1.3$ ) sources. Inner source PIs are quite prominent around  $W \approx 1$  and their narrow width (resulting from strong adiabatic cooling) indicates that they were produced close to the Sun. The highest density is reached close to, or slightly below,  $W = 1$ . This is

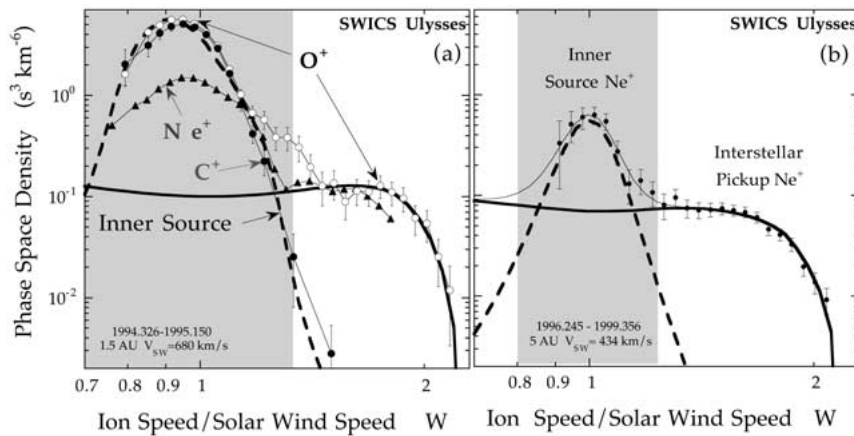


Figure 2. (a) Distribution functions of  $O^+$ ,  $C^+$  and  $Ne^+$  measured with SWICS on *Ulysses* at  $\sim 1.5$  AU from  $\sim -60^\circ$  to  $+60^\circ$  latitude. Interstellar  $O^+$  and  $Ne^+$  (but not  $C^+$ ) are observed above  $W \sim 1.4$ . The density peaks below  $W \approx 1.4$  are attributed to pickup ions from the inner source whose velocity distribution is modeled by the bold dashed curve. The inner source distributions of  $C^+$ ,  $O^+$ , and  $Ne^+$  reach maximum values somewhat below  $W = 1$  and are relatively narrow, implying that their sources are close to the Sun and that pitch angle scattering is weak. (b) Averaged velocity distribution of  $Ne^+$  at around 5 AU and between about  $+30^\circ$  and  $\sim -40^\circ$  latitude. Even at this larger distance inner source  $Ne^+$ , while less prominent than at 1.5 AU is nevertheless clearly visible. Because of additional adiabatic cooling, the inner source distribution is narrower at 5 AU compared to 1.5 AU and the peak is now centered at  $W = 1$ , as expected for a nearly azimuthal magnetic field direction.

consistent with weak pitch angle scattering at  $90^\circ$  and a large ( $\sim 1$  AU) scattering mean free path. By fitting inner source model distributions to the observed spectra (Schwadron *et al.*, 2000), it is possible to deduce the approximate radial profile of the neutrals that produce the inner source PIs. Best fits of interstellar model distributions (e.g., Gloeckler and Geiss, 1998) to the measured distribution functions above  $W \approx 1.5$  yield both the ionization rate and the density of the parent neutral species. The bold dashed and bold solid curves of Figure 2 are the respective fits for  $O^+$  (left panel) and  $Ne^+$  (right panel).

The radial profiles of the density of neutral oxygen and pickup  $O^+$  are derived by fitting inner source and interstellar model curves respectively to the  $O^+$  spectrum of Figure 2(a). The results are shown in Figure 3. The density of inner source neutrals at low latitudes peaks close to the Sun ( $\sim 20$  solar radii) and the resulting pickup ion density beyond  $\sim 0.15$  AU decreases as  $1/R^2$ , where  $R$  is the distance from the Sun. Inner source  $O^+$  dominates the inner heliosphere to about 1 AU, while interstellar  $O^+$  become more abundant beyond a few AU and their total mass in the heliosphere far exceeds that of the inner source  $O^+$ . It would not be surprising if the radial profiles of the density of inner source pickup ions (and neutrals) would vary with time (or solar activity) and latitude. This possibility is now being examined.

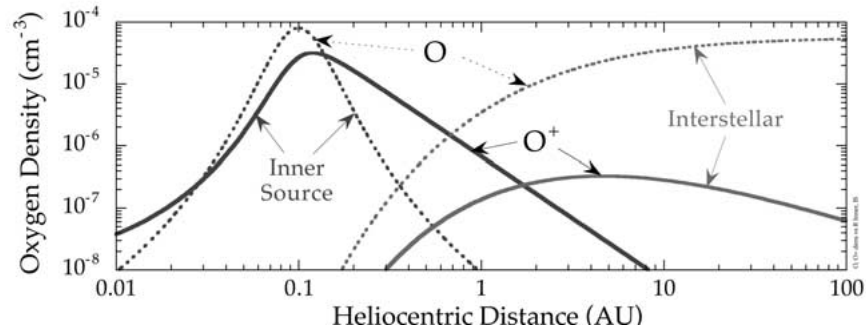


Figure 3. Low latitude radial profiles of the densities of atomic oxygen (dotted curves) and the resulting pickup  $O^+$  (bold curves) derived from the  $O^+$  velocity distribution of Figure 2(a). The inner source neutral density peaks at about 0.1 AU ( $\sim 20$  solar radii) and has a FWHM width of  $\sim 0.06$  AU. Inner source C has a similar radial profile.

### 3. Composition of Pickup Ions

The chemical composition of pickup ions from the two sources can be estimated from the measured distribution functions or from the mass per charge ( $m/q$ ) distribution selected according to the  $W$  range where the respective pickup ion population predominates (see Figures 1 and 2). The  $m/q$  histogram of low latitude inner source PIs and of IPIs is displayed in Figure 4. The left panel shows the composition of inner source pickup ions ( $0.8 < W < 1.15$ ) observed at low latitudes during a one year period. C and O are the two prominent ions with smaller abundance of N, Ne, and Mg. Three molecular species ( $CH^+$ ,  $OH^+$ , and  $H_2O^+$ ) are also identified, although not well resolved from the more abundant neighboring ions. Mass 28 ( $Si^+$  and  $CO^+$ ) has also been observed (Gloeckler *et al.*, 2000a) but is not shown here. Higher masses are outside the  $m/q$  range of SWICS.

The composition of interstellar pickup ions consists of high-FIP elements and their isotopes ( $H^+$ ,  $^3He^+$ ,  $^4He^+$ ,  $^4He^{++}$ ,  $N^+$ ,  $O^+$ ,  $^{20}Ne^+$ , and  $^{22}Ne^+$ ).  $Ar^+$ , also expected to be present is outside the mass range of the SWICS instrument and has as yet not been detected. It is these same elements that are found in the Anomalous Cosmic Rays (ACRs) (e.g. Cummings *et al.*, 1999). This, as well as other evidence (see Gloeckler and Wenzel, 2001), shows that IPIs are the source of the ACRs. In Figure 4b, showing IPIs with masses above 10, there appear to be, in addition to the high FIP elements, water group molecules ( $OH^+$  and  $H_2O^+$ ) at a few percent level. Some fraction of these, as well as all the  $C^+$  are likely to be spill-over of residual inner source ions that have  $W > 1.3$ . The rest of  $OH^+$  and  $H_2O^+$  is probably produced by degassing of interstellar and interplanetary dust and planetary material at distances of several AU.

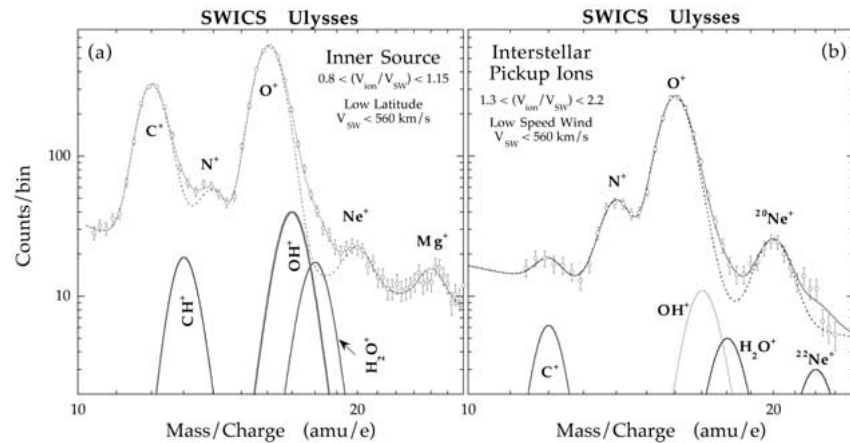


Figure 4. Running average of the counts per mass/charge bin versus mass/charge for inner source (a) and interstellar (b) PIs with speeds in the indicated  $W$  (ion speed/solar wind speed) ranges. These data were collected during long time periods when the solar wind speed was below  $560 \text{ km s}^{-1}$  (March 1, 1996 to March 1, 1997 for the inner source and January 1, 1997 to January 1, 2000 for the IPIs). The exact shapes of the peaks for  $\text{C}^+$  and  $\text{O}^+$  were obtained when SWICS traversed the distant plasma tail of comet Hyakutake (Gloeckler *et al.*, 2000b) and detected copious amounts of cometary  $\text{C}^+$ ,  $\text{N}^+$ ,  $\text{O}^+$  and water group molecular ions. Dotted curves are fits to the data assuming no contributions from molecules.

#### 4. Pickup Ions as Sources of Accelerated Particles

From velocity distributions similar to those shown in Figures 1 and 2, we have obtained densities of interstellar atoms at the heliospheric termination shock using ionization rates derived from the respective shapes of the pickup ion distribution functions. Our results for the densities of interstellar atomic N, O, and Ne based on analysis of additional SWICS data, along with our previous values for H and He (Gloeckler *et al.*, 1997) are summarized in column 2 of Table I. The density ratios of inner source pickup ions derived from data of Figure 4(a) are compared to the corresponding ratios of the solar wind and of MeV particles accelerated in Corotating Interaction Regions (CIR) in Figure 5(a). It is evident that the compositions of all three populations are comparable to within a factor of two. This implies that both the solar wind and inner source PIs are probable sources for CIR accelerated particles as was suggested previously (e.g., Gloeckler *et al.*, 2000c).

In Figure 5(b) we compare the elemental abundance relative to O of Anomalous Cosmic Rays with that of PIs at the termination shock. Almost all of H, He, N, O, and Ne are IPIs. C, Mg, and Si are far less abundant and all come from the inner source. With the exception of H and He, the composition of these two populations is similar, suggesting not only that IPIs are the source of the main component of ACRs (H, He, N, O, and Ne) but also that the inner source PIs are the likely source of the minor ACRs such as C, Mg, and Si. Because of adiabatic cooling, inner source PIs produced close to the Sun would have very peaked velocity dis-

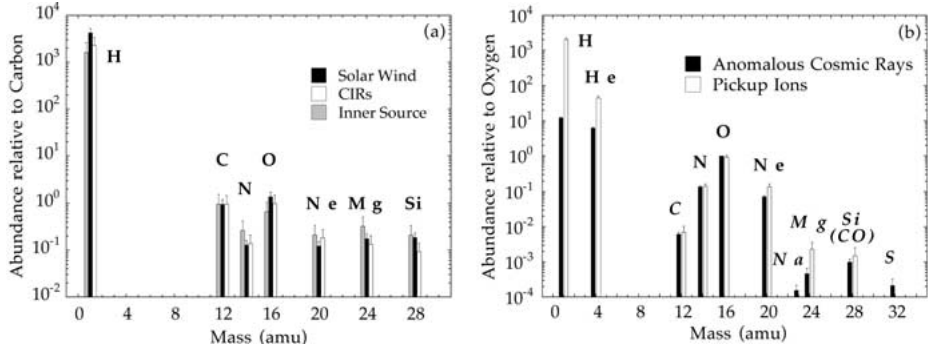


Figure 5. (a) Comparison of abundances relative to carbon of solar wind ions (from von Steiger *et al.*, 2000), of inner source pickup ions (present work) and  $\sim$  MeV particles in CIRs (compiled by Gloeckler and Wenzel, 2001). (b) Comparison of abundances relative to oxygen of Anomalous Cosmic Rays (e.g., Cummings *et al.*, 1999) and pickup ions. The densities of inner source PIs were extrapolated to the termination shock using radial profiles such as shown in Figure 3 and then added to the IPI densities derived from atomic densities at the termination shock (column 2 in Table 1) and the respective production rates.

TABLE I

Densities of atoms at the heliospheric termination shock ( $\sim 85$ – $\sim 110$  AU) and densities of atoms and ions in the local interstellar cloud

Iso- tope	Density at termination shock ( $\text{cm}^{-3}$ )	Filtration factor	Ion fraction	Densities in the local interstellar cloud ( $\text{cm}^{-3}$ )			Local cloud to solar system ratio <sup>a</sup>
				Atoms	Ions	Total	
$^1\text{H}$	$0.115 \pm 0.015$	0.58	0.18	0.20	0.043	0.243	1
$^4\text{He}$	$0.0153 \pm 0.002$	1	0.37	0.0153	0.0090	0.0243	1
$^3\text{He}$	$(3.8 \pm 1.0) \times 10^{-6}$	1	0.37	$3.8 \times 10^{-6}$	$2.2 \times 10^{-6}$	$6.0 \times 10^{-6}$	–
$^{14}\text{N}$	$(8.0 \pm 1.3) \times 10^{-6}$	0.92	0.41	$8.7 \times 10^{-6}$	$6.0 \times 10^{-6}$	$1.47 \times 10^{-5}$	$0.63 \pm 0.20$
$^{16}\text{O}$	$(5.6 \pm 0.8) \times 10^{-5}$	0.82	0.27	$6.8 \times 10^{-5}$	$2.5 \times 10^{-5}$	$9.3 \times 10^{-5}$	$0.48 \pm 0.18$
$^{20}\text{Ne}$	$(9.2 \pm 2.0) \times 10^{-6}$	1	$>0.7$	$9.2 \times 10^{-6}$	$>2.15 \times 10^{-5}$	$>3.07 \times 10^{-5}$	$\geq 1$

<sup>a</sup>Solar System abundances are taken from Grevesse and Sauval (1998).

tributions at  $W = 1$  in the outer heliosphere and would thus not be expected to be efficiently injected for acceleration to ACR energies by the termination shock, contrary to observations. Pre-acceleration of inner source PIs during their transport to the termination shock would be required to overcome strong adiabatic losses and thus increase the injection efficiency of these accelerated inner source PIs to levels comparable to that for the IPIs. Preferential acceleration of pickup (compared to solar wind) ions has been observed both in the quiet solar wind and in association with CIRs (Gloeckler *et al.*, 2000c). The fact that He and especially H are underabundant in the ACRs compared to interstellar pickup ions is generally attributed to the poor injection efficiency for these light elements. Realistic models of shock

acceleration must be able to account for the mass-dependent injection efficiency observed.

## 5. Characteristics of the Local Interstellar Cloud

### 5.1. PHYSICAL CHARACTERISTICS

From measurements of IPIs we can derive the composition at the termination shock of atoms entering from the LIC (column 2 in Table 1). This composition differs from that of the gas in the LIC because of an effect known as filtration, a reduction in the density of those atoms that have a sufficiently high charge-exchange cross section with slow-moving, hot protons in the filtration region between the heliopause and the interstellar bow shock (e.g., Gloeckler *et al.*, 1997). The elements affected by filtration are H, O, and N, but not the noble gases He and Ne. The reduction of the density of atomic H by filtration (column 3) may be derived using the average atomic H/He in the LIC, obtained from column density measurements of EUV absorption from nearby white dwarf stars, and the H and He densities at the termination shock from column 2 in Table 1. The filtration factors of N and O are then obtained from the filtration of H using their respective charge-exchange cross sections with protons (for details see Gloeckler *et al.*, 2001). The filtration factor of H is used to derive the proton density in the filtration region, and the LIC proton density is obtained by reducing its density in the filtration region by the bow shock compression ratio, believed to be around 2 (Gloeckler *et al.*, 1997). The resulting ionization fractions of H and He (derived using the LIC atomic He density and the universal total H/He ratio of 10), listed in column 4 in Table 1, are taken from Gloeckler *et al.* (1997). For N and O we adopt values obtained by Slavin and Frisch (2001), using the CLOUDY model (cf., Frisch and Slavin, 1996). The CLOUDY model gives a very high ion fraction for neon. Thus, in the case of Ne the ion density which is only obtained theoretically, dominates the total density. For this reason and because the solar abundance of neon is poorly known, we give only a lower limit for the ionization fraction of neon. The total density of the LIC gas is  $0.27 \text{ cm}^{-3}$ , and the total ionization fraction of the gas is 0.16, making it a fairly neutral gas.

The temperature of neutral H and He in the LIC may be estimated from model fits to EUV backscatter radiation from interstellar atomic H and He ionized in the heliosphere (e.g., Bertaux *et al.*, 1985; Chassefière *et al.*, 1988). Due to effects of filtration, this method gives upper limits for the LIC atomic H temperature. The most accurate determination of the He temperature ( $7000 \pm 600 \text{ K}$ ) comes from direct measurements of the distribution of flow vectors of interstellar He with *Ulysses* (Witte *et al.*, 1996). A third technique for estimating the temperature of LIC atoms uses measurements of the spatial distribution of the corresponding pickup ions (e.g. Möbius *et al.*, 1995). This method, as yet applied only to He,



is illustrated in Figure 6 where we show the running averaged counting rate of  $\text{He}^+$  (proportional to phase space density) measured with SWICS on ACE as a function of time. The prominent peaks in the  $\text{He}^+$  density observed in late 1998 and 1999 reflect the profile of the density of interstellar atomic He which increases to reach a maximum in the direction exactly opposite to the inflow direction of the interstellar gas, a position reached by ACE on about December 5 (DOY 339) of each year. From model fits to the  $\text{He}^+$  density peaks it is possible to obtain the total loss rate,  $\beta_{\text{loss}}$  of He for various values of the LIC He temperature,  $T$ . The best values of  $\beta_{\text{loss}}$  (with  $T$  fixed at 7500 K) obtained in this fashion for 1998 and 1999 are listed next to each peak in Figure 6. The total loss rates are about 60% higher than the measured He photo-ionization rates for the respective years (McMullin, private communication) and the increase of  $\beta_{\text{loss}}$  from 1998 to 1999 is most likely due to increased solar activity. The  $\sim 60\%$  higher loss rates we obtain imply that the contribution to  $\beta_{\text{loss}}$  from electron impact ionization of atomic He is large, consistent with other estimates of the total He loss rate (Witte *et al.*, 1996; Rucinski *et al.*, 1996; Gloeckler and Geiss, 1998). Increasing the value of  $T$  by as much as 2000 K above that obtained from direct measurements of He taken in 1990–1992 (Witte *et al.*, 1996) does not significantly improve the fits in the cone regions. The deviations of the measured  $\text{He}^+$  rate in the focusing peaks from model predictions are easily accounted for by variations in the production rate of pickup  $\text{He}^+$  as seen outside the focusing cone regions, suggesting that cross field diffusion, which would broaden the peaks, is not significant for pickup  $\text{He}^+$ .

## 5.2. CHEMICAL PROPERTIES

Column 7 of Table 1 lists the total densities of elements in the LIC. Probably only a relatively small fraction (20–30% for O, somewhat less for N and negligible amounts for H, He, and Ne) of the elements listed in Table I is contained in grains (Grün and Švestka, 1996) and we have not included these contributions in column 7. The last column gives the ratios of abundances (normalized to He) of the elements in the LIC to that in the Solar System, taken to represent the elemental composition in the protosolar cloud 4.5 Gyrs ago. It appears that the heavy elements N and O in the present-day LIC are underabundant compared to their abundance in the protosolar cloud. Wielen and Wilson (1997) also report a Fe/H ratio for nearby stars of solar age which is 1.48 times lower than the solar ratio. All of this is just the opposite to expectations. Galactic evolution over the last 4.5 Gyrs should have enriched the abundance of heavy elements in the LIC gas compared to that in the Solar System, contrary to what is observed. On the other hand, the abundance of neon in the LIC appears to be equal or even higher than the solar abundance, which would be more consistent with expectation. However, before drawing a definite conclusion about the LIC abundance of neon, we intend to further study the ion fraction of Ne in the LIC and the Ne abundance in the Sun.

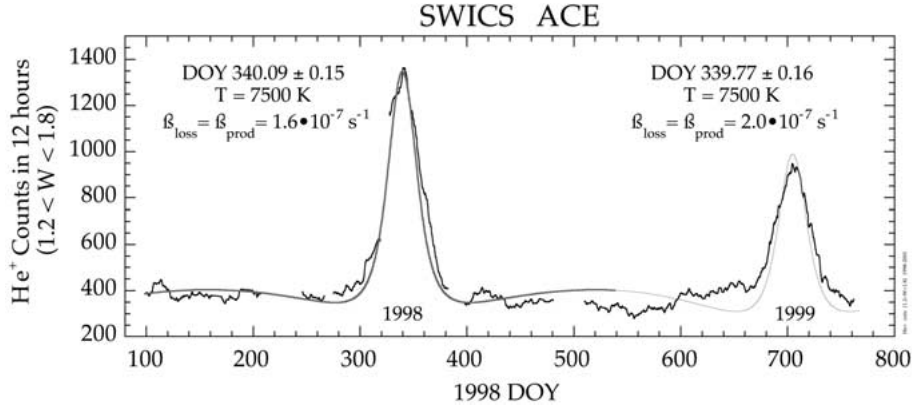


Figure 6. Variation of the 31-day running average of pickup  $\text{He}^+$  rate (counts per 12 hours) observed with SWICS on the Advanced Composition Explorer Spacecraft (ACE) during a  $\sim 22$ -month period. ACE is in interplanetary space upstream of Earth at 1 AU. Each year in early December (DOY  $\approx 339$ ) ACE passes through the He focusing cone, a high density region of interstellar He atoms directly opposite to the inflow direction of the LIC gas. This high density region results from gravitational focusing of neutral He. The shape of the focusing cone profile is approximately gaussian and depends primarily on the He ionization rate ( $\beta_{\text{loss}}$ ), and temperature. Smooth curves are model calculations using a fixed temperature  $T$  of 7500 K and adjusting  $\beta_{\text{loss}}$  to fit the data. The 15% to 25% deviation of the measured  $\text{He}^+$  rate from the model curve is most likely due to variations of the production rate of pickup  $\text{He}^+$  from the average rate  $\beta_{\text{prod}}$  which, in the model, was taken to be equal to  $\beta_{\text{loss}}$ .

## 6. Characteristics of the Inner Source

There are probably several different sources from which inner source PIs are produced. One likely source is neutrals evaporated from interstellar grains at distances of several AU or less from the Sun which could produce some of the pickup  $\text{C}^+$  and  $\text{O}^+$  (Geiss *et al.*, 1996). But the discovery of inner source  $\text{Ne}^+$  (Gloeckler *et al.*, 2000a) suggested that another major source for inner source pickup ions was the ‘recycled’ solar wind. This source of neutrals is located at around 20 solar radii (Figure 3). It appears that here, solar wind particles, absorbed by grains are released and after being ionized are picked up by the solar wind (Gruntman, 1996; Schwadron *et al.*, 2000). The number of solar wind particles converted in this way into low charge ions depends on dust properties, in particular their trajectories. If we experimentally identify a source region of a pickup ion species produced by the interaction of the solar wind with grains, then the production rate  $Q(r_1)$  per unit area is governed by the macroscopic cross section

$$\Sigma(r_1) = \frac{1}{\Delta r} = \int_a^b \int \sigma(\rho) n(\rho, r) d\rho dr, \quad (1)$$

where  $r_1$  is the distance of the source region from the solar center,  $\Delta r$  is its width,  $a = r_1 - \Delta r/2$ ,  $b = r_1 + \Delta r/2$ ,  $\rho$  is the grain radius and  $\sigma$  its cross section for

solar wind absorption, and  $n(\rho, r)$  is the grain number density with radii between  $\rho$  and  $\rho + d\rho$ . We distinguish two limiting cases:

### I. *The Steady State Model*

We assume that solar wind absorption is in equilibrium with release. Then the production rate per unit area of pickup ion species  $i$  at  $r_1$  is

$$Q_1^i = \Sigma(r_1) \Delta r f_{\text{sw}}^i(r_1), \quad (2)$$

where is  $f_{\text{sw}}^i$  the flux of the solar wind species  $i$  under consideration.

### II. *The Poynting–Robertson Model*

The time  $t_{\text{P-R}}$  for a dust particle at a heliocentric distance  $r$  to spiral into the Sun due to the Poynting–Robertson effect is given by

$$t_{\text{P-R}} = c_1 r^2 \quad (3)$$

(cf., Allen, 1976, p. 157 for  $c_1$ ). For a black spherule  $t_{\text{P-R}}$  is  $\sim 10^3$  years at 1 AU and  $\sim 10$  years at 20 solar radii. Differentiation of (3) gives the radial Poynting–Robertson speed

$$V_{\text{P-R}}(r) = (2c_1 r)^{-1}. \quad (4)$$

Assuming there is no loss outside the interval  $\Delta r$  and assuming  $f_{\text{sw}}^i \sim r^{-2}$ , the number of accumulated atoms of the solar wind species  $i$  between its starting radius  $r_2$  and  $r_1$  is given by

$$N^i = 2\Sigma(r_1) c_1 r_1^2 f_{\text{sw}}^i(r_1) \ln(r_2/r_1). \quad (5)$$

The grains pass through the interval  $\Delta r$  in the time  $\tau = \Delta r / V_{\text{P-R}}(r_1)$ . If the accumulated particles are released in this interval, the production rate per unit area of PIs is given by

$$Q_{\text{II}}^i = N^i V_{\text{P-R}} \quad (6)$$

or

$$Q_{\text{II}}^i = \Sigma(r_1) r_1 f_{\text{sw}}^i(r_1) \ln(r_2/r_1). \quad (7)$$

Thus the ratio of the production rates by model II and model I is

$$Q_{\text{II}}^i / Q_1^i = (r_1 / \Delta r) \ln(r_2/r_1). \quad (8)$$

For grains starting in the asteroid belt at  $r_2 \sim 600 R_{\text{Sun}}$ , and for  $r_1 = 20 R_{\text{Sun}}$  and  $\Delta r = 10 R_{\text{Sun}}$ , we obtain  $Q_{\text{II}}^i / Q_1^i = 6.8$ .

The expressions for PI production rates as given in Equations (7) and (8) are independent of many uncertain parameters. Factors that govern the Poynting–Robertson effect such as grain sizes, densities and optical properties are contained

in  $c_1$ , and these cancel, because  $V_{P-R} = (2c_1r)^{-1}$  cancels for  $Q_{II}^i$  (Equation (7)). When comparing the pickup ion production rates for the steady state model and the Poynting–Robertson model,  $\Sigma(r_1)$  and  $f_{sw}^i(r_1)$  also cancel, so that  $Q_{II}^i/Q_I^i$  depends only on trajectory parameters of the dust particles.

Models I and II are for bound orbits. The resulting relationships between the pickup ion production rates  $Q$  and the macroscopic cross sections  $\Sigma$  differ by an order of magnitude (Equation (8)). The orbits of interstellar grains, some  $\beta$ -meteorites (Grün *et al.*, 1985), and grains from long-period comets are on approximately hyperbolic orbits. For grains on such trajectories production rates could be even lower than those obtained for model I (Equation (2)).

$Q_I$  and  $Q_{II}$  depend on the macroscopic cross section for solar wind interaction. The mechanism of release, diffusion or sputtering, does not enter. Mann (private communication) has pointed out that grain-grain collisions could contribute to the inner source pickup ions. The models presented here can be adapted to include this mechanism by taking into account the grain sizes and trajectories before the collision. We note that collisions will also release intrinsic grain material. This is important when interpreting the refractory elements among the inner source pickup ions.

At  $r_1 = 20$  solar radii, the steady state model I should be applicable for the most volatile elements such as He and Ne. On the other hand, particles collecting solar wind ions on Poynting–Robertson trajectories could contribute to inner source pickup ions in the case of refractory elements.

In combination with other evidence, pickup ion data could contribute to constraining dust densities and trajectories in the innermost heliosphere, especially if source regions of different pickup ion species are identified near the Sun and compared.

## 7. Acknowledgements

This work was supported, in part, by NASA/JPL contract 955460. Special appreciation for the effort to develop the SWICS/*Ulysses* instrument and to analyze the data presented here goes to E. O. Tums and C. Gloeckler, respectively.

## References

- Allen, C. W.: 1976, *Astrophysical Quantities*, 3rd edition, The Athlone Press, London.
- Axford, W. I.: 1972, in C. P. Sonett, P. J. Coleman Jr., and J. M. Wilcox, (eds.), *Proc. Solar Wind Conf.*, Asilomar, California, 1971, NASA **SP-308**, 609.
- Bertaux, J.-L., Lallement, R., Kurt, V. G., and Mironova, E. N.: 1985, *Astron. Astrophys.* **150**, 1.
- Chassefière, E., Dalaudier, F., and Bertaux, J.-L.: 1988, *Astron. Astrophys.* **201**, 113.
- Cummings, A. C., Stone, E. C., and Steenberg, C. D.: 1999, *Proc. 26th Int. Cosmic Ray Conf.*, Utah **7**, 531.

- Fisk, L. A., Kozlovsky, B., and Ramaty, R.: 1974, *Astrophys. J.* **190**, L35.
- Frisch, P. C. and Slavin, J. D.: 1996, *Space Sci. Rev.* **78**, 223.
- Geiss, J., Gloeckler, G., Mall, U., von Steiger, R., Galvin, A. B., and Ogilvie, K. W.: 1994, *Astron. Astrophys.* **282**, 924.
- Geiss, J., Gloeckler, G., Fisk, L. A., and von Steiger, R.: 1995, *J. Geophys. Res.* **100**, 23 373.
- Geiss, J., Gloeckler, G., and von Steiger, R.: 1996, *Space Sci. Rev.* **78**, 43.
- Gloeckler, G. and Geiss, J.: 1998, *Space Sci. Rev.* **86**, 127.
- Gloeckler, G. *et al.*: 1992, *Astron. Astrophys. Suppl. Ser.* **92**, 267.
- Gloeckler, G. *et al.*: 1993, *Science* **261**, 70.
- Gloeckler, G., Schwadron, N. A., Fisk, L. A., and Geiss, J.: 1995, *Geophys. Res. Lett.* **22**, 2665.
- Gloeckler, G., Fisk, L. A., and Geiss, J.: 1997, *Nature* **386**, 374.
- Gloeckler, G., Fisk, L. A., Geiss, J., Schwadron, N. A., and Zurbuchen, T. H.: 2000a, *J. Geophys. Res.* **105**, 7459.
- Gloeckler, G. *et al.*: 2000b, *Nature* **404**, 576.
- Gloeckler, G., Fisk, L. A., Zurbuchen, T. H., and Schwadron, N. A.: 2000c, in R. A. Mewaldt, J. R. Jokipii, M. A. Lee, E. Möbius, and T. H. Zurbuchen (eds.), *Acceleration and Transport of Energetic Particles Observed in the Heliosphere*, AIP Conf. Proceedings No. 528, p. 221.
- Gloeckler, G., Geiss, J. and Fisk, L. A.: 2001, in A. Balogh, E. J. Smith, and R. G. Marsden, (eds.), *The Heliosphere near Solar Minimum: the Ulysses Perspectives*, Springer-Praxis, Berlin, in press.
- Gloeckler, G., and Wenzel, K.-P.: 2001, in J. Bleeker, J. Geiss, M. C. E. Huber, and A. Russo, (eds.), *The Century of Space Science*, Kluwer Academic Publishers, Dordrecht, in press.
- Grevesse, N. and Sauval, A. J.: 1998, *Space Sci. Rev.* **85**, 161.
- Grün, E., Zook, H. A., Fechtig, H., and Giese, R. H.: 1985, *Icarus* **62**, 244.
- Grün, E. and Švestka, J.: 1996, *Space Sci. Rev.* **78**, 347.
- Gruntman, M.: 1996, *J. Geophys. Res.* **101**, 15555.
- Möbius, E., Hovestadt, D., Klecker, B., Scholer, M., Gloeckler, G., and Ipavich, F. M.: 1985, *Nature* **318**, 426–429, 1985.
- Möbius, E., Rucinski, D., Hovestadt, D., and Klecker, B.: 1995, *Astron. Astrophys.* **304**, 505.
- Rucinski, D., Cummings, A. C., Gloeckler, G., Lazarus, A. J., Möbius, E., and Witte, M.: 1996, *Space Sci. Rev.* **78**, 73.
- Schwadron, N. A., Geiss, J., Fisk, L. A., Gloeckler, G., Zurbuchen, T. H., and von Steiger, R.: 2000, *J. Geophys. Res.* **105**, 7465.
- Slavin, J. D. and Frisch P. C.: 2001, *Astrophys. J.* (in press).
- Vasyliunas, V. M. and Siscoe, G. L.: 1976, *J. Geophys. Res.* **81**, 1 247.
- von Steiger, R. *et al.*: 2000, *J. Geophys. Res.* **105**, 27217.
- Wielen, R. and Wilson: 1997, *Astron. Astrophys.* **306**, 505.
- Witte, M., Banaszkiwicz, M., and Rosenbauer, H.: 1996, *Space Sci. Revs.* **78**, 289.